

## A direct XFEM formulation for modeling of cohesive crack growth in concrete

J. L. Asferg<sup>†</sup>, P. N. Poulsen<sup>‡</sup> and L. O. Nielsen<sup>††</sup>

*Department of Civil Engineering, Technical University of Denmark, DK-2800 Kgs. Lyngby, Denmark  
(Received August 17, 2006, Accepted February 5, 2007)*

**Abstract.** Applying a direct formulation for the enrichment of the displacement field an extended finite element (XFEM) scheme for modeling of cohesive crack growth is developed. Only elements cut by the crack is enriched and the scheme fits within the framework of standard FEM code. The scheme is implemented for the 3-node constant strain triangle (CST) and the 6-node linear strain triangle (LST). Modeling of standard concrete test cases such as fracture in the notched three point beam bending test (TPBT) and in the four point shear beam test (FPSB) illustrates the performance. The XFEM results show good agreement with results obtained by applying standard interface elements in FEM and with experimental results. In conjunction with criteria for crack growth local versus nonlocal computation of the crack growth direction is discussed.

**Keywords:** extended finite elements-XFEM; fracture mechanics; cohesive crack growth.

---

### 1. Introduction

Throughout the last century research has been carried out regarding methods to determine the ultimate strength of reinforced concrete structures. Today well-documented methods are available for estimating the ultimate strength of most reinforced concrete (RC) structures and the theory of rigid plasticity is highly developed (e.g. Nielsen 1999). However, most of these methods require the use of empirical factors and do not consider phenomena such as size effects and reinforcement arrangement in a fully consistent way. Regarding RC structures in the serviceability limit state the predictive capability of existing methods of analysis is limited. Predictions regarding the development in e.g., stiffness due to cracking, development in crack widths and the deformations at ultimate loading for RC structures are often based on empiric rules.

A consistent model for modeling of RC structures may be obtained if the model is able to predict the cracking that takes places long before the ultimate capacity of RC structures is reached. Cracking influences structural properties and is one of the governing factors in relation to durability and service life prediction. A consistent approach for modeling of concrete may be based on the concept of fracture mechanics and the capability to model localized crack growth. Aiming at the capability to model real size RC structures with complex shapes it would be beneficial if the model fits within the concept of the finite element method (FEM) and that the method do not require to

---

<sup>†</sup>Corresponding Author, E-mail: [jla@byg.dtu.dk](mailto:jla@byg.dtu.dk)

<sup>‡</sup>E-mail: [pnp@byg.dtu.dk](mailto:pnp@byg.dtu.dk)

<sup>††</sup>E-mail: [lon@byg.dtu.dk](mailto:lon@byg.dtu.dk)

dense FEM meshes.

Concrete belongs to the group of materials that are classified as being quasi-brittle (e.g. Karihaloo 1995) and a suitable model for crack propagation in concrete is the fictitious crack model by Hillerborg, *et al.* (1976) that models the crack propagation within the framework of cohesive cracking (Barenblatt 1962, Dugdale 1960).

Today several commercial FEM codes have interface elements suitable for modeling of discrete cohesive cracks. The use of interface elements however requires the crack path to be known beforehand and is therefore less relevant when the aim is to predict crack patterns. Several programs also have elements for smeared cracking that are based on the concept of a crack band (Bažant and Oh 1983) however the smeared approach is not well-suited for modeling of localized crack growth.

Remeshing has been used as a tool when modeling crack growth, (Bouchard, *et al.* 2000, 2002, Patzák and Jirásek 2004). Remeshing is however cumbersome hence it requires projection of variables between different meshes. Three methods: the element free Galerkin method (Belytschko, *et al.* 1996), the embedded crack methods (e.g. Jirásek 2000) and the extended finite element method (XFEM) (Belytschko and Black 1999) allow modeling of crack growth without remeshing. While the element free Galerkin method deviates in its principal structure from the structure of commercial FEM codes, embedded cracks and the XFEM fits well in the structure of commercial FEM codes. The XFEM is however preferable to the concept of embedded cracks hence in the XFEM the strains are independent in the separated parts of the elements whereas they are partly coupled in the embedded concept (Jirásek and Belytschko 2000).

In the extended finite element method the displacement field consists of two parts, a continuous and a discontinuous part. The continuous part is the standard displacement field corresponding to the situation without any cracks. The discontinuous displacement field is based on local partitions of unity (Melenk and Babuška 1996) and enables the element to include a discontinuity, in the present case a cohesive crack.

XFEM has been applied to different problems within the area of fracture mechanics. While it was first developed for linear elastic fracture mechanics (Belytschko and Black 1999, Moës, *et al.* 1999, Stolarska, *et al.* 2001) it has now been applied to different problems such as cohesive cracking (Wells and Sluys 2001, Moës and Belytschko 2002, Zi and Belytschko 2003, Mergheim, *et al.* 2005) arbitrary branched and intersecting cracks (Daux, *et al.* 2000) and three dimensional crack propagation (Sukumar, *et al.* 2000). Reference is also made to Karihaloo and Xiao (2002) for an overview of the earlier works regarding the XFEM.

Considering linear elastic fracture mechanics (Belytschko and Black 1999, Moës, *et al.*, 1999, Stolarska, *et al.* 2001) nodes in elements fully cut by the discontinuity was enriched by the step function while the tip element was enriched with an asymptotic field. In cohesive crack models, cohesive stresses act near the crack tip and it is assumed that no singularity is present at the crack tip. However, considering partly cracked elements for cohesive crack growth Moës and Belytschko (2002) enriched the crack tip element with a set of nonsingular branch functions to model the displacement field around the tip of the discontinuity. Wells and Sluys (2001) considered fully cracked elements and applied the Heaviside step function as the only enrichment of nodes with a supporting side cut by the discontinuity. Applying the Heaviside step function as in Wells and Sluys (2001) the nodal enrichment influences not only the displacement field in the elements cut by the discontinuity but also in the elements sharing the enriched nodes, i.e., the enrichments typically have to be dealt with in a band of three elements along the line of the discontinuity.

Zi and Belytschko (2003) proposed an enrichment of the crack tip element for the case of partly

cracked elements in which the shifted sign function was applied. The application of the shifted sign function to a 1D example is illustrated in Fig. 1(b). As shown the enrichment only influences elements cut by the discontinuity. In Mergheim, *et al.* (2005) a dual node strategy was applied and the displacement field was not decomposed into a continuous and discontinuous part in the same way as in the approach by Wells and Sluys (2001) and Zi and Belytschko (2003). However even though the basis for the shape functions is different the scheme in Mergheim, *et al.* (2005) is able to model the same variation in the displacement field as in the scheme by Zi and Belytschko (2003). The enrichment as applied by Mergheim, *et al.* (2005) is illustrated in Fig. 1(c). Although the authors in Mergheim, *et al.* (2005) distinct their approach from the XFEM it is essentially based on the same concept.

In the present paper a direct XFEM scheme for modeling of cohesive crack growth is developed using the Heaviside step function and limiting the discontinuous displacement field to elements cut by the crack. The XFEM formulation follows the concepts proposed in Asferg, *et al.* (2004). The Heaviside step function,  $H$ , is applied as the only enrichment of elements cut by the discontinuity c.f. Fig. 1(a).

Fig. 1 illustrates how a displacement jump of the magnitude of one may be modeled applying the three different approaches discussed above. For the present approach and the approach by Zi and Belytschko (2003) the two upper sketches illustrate the continuous displacement fields for node 1 respectively node 2 while sketch 3 and 4 illustrate the discontinuous displacement fields. Regarding the approach by Mergheim, *et al.* (2005) the two upper figures illustrate the displacement field for the two “original” nodes 1 and 2 while Figs. 3 and 4 depict the displacement fields for the dual nodes 1\* and 2\*. Finally the lower sketch in each row depicts an example of a displacement field containing a jump of the magnitude of one. From Fig. 1 it is evident that the difference between the three approaches is a question about the applied basis for modeling the displacement field. Compared to the enrichment by the shifted sign function in Zi and Belytschko (2003) and the enrichment in Mergheim, *et al.* (2005) the proposed enrichment is more straight forward but essential the three formulations models the same discontinuous field.

Common for the approaches in Wells and Sluys (2001), Moës and Belytschko (2002), Zi and Belytschko (2003), Mergheim, *et al.* (2005) is that they all adopt a nonlocal approach for the determination of the crack growth direction. A nonlocal approach is required because of the lack of capability of the tip element to model equal stresses at both sides of the discontinuity which is most pronounced when CST elements are considered.

The suggested XFEM scheme fits in the context of standard FEM code and it is applied to the 3-node constant strain triangle elements (CST) and the 6-node linear strain triangle elements (LST). The performance of the scheme is illustrated by modeling of fracture in concrete benchmark tests such as the three point beam bending test (TPBT) and the four point shear beam test (FPSB). In the present work only elements completely cut by a crack have been considered, i.e., the crack extends element by element and the crack tip will always be located on an element edge.

In section two the enrichment of the displacement field will be introduced and the discontinuous displacement fields developed and illustrated for CST and LST elements. Section three concerns the variational formulation while matters of the implementation is discussed in section four. Section five shows the numerical examples.

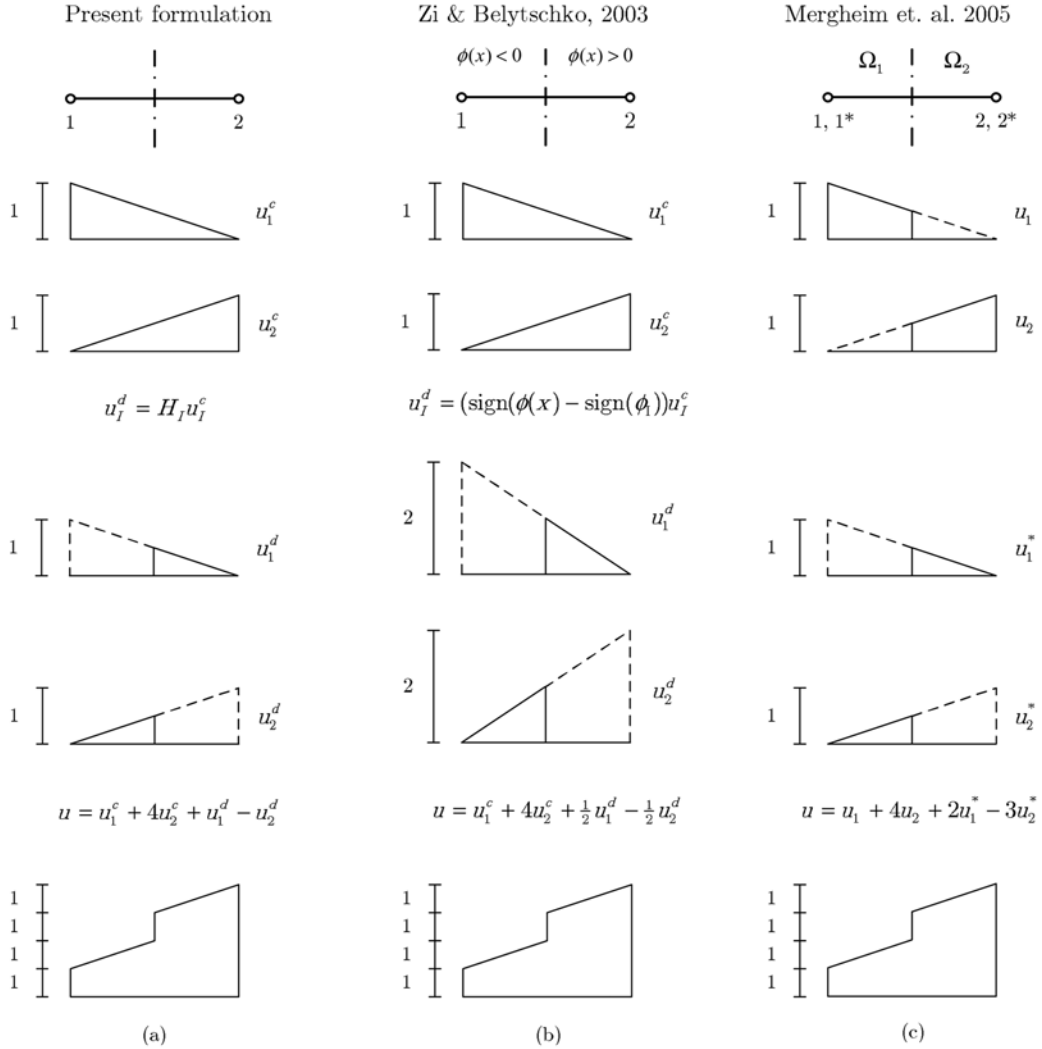


Fig. 1 Comparison of different enrichments of the displacement field: (a) Present formulation, (b) Zi and Belytschko (2003), (c) Mergheim, *et al.* (2005). For the present formulation and the formulation by Zi and Belytschko (2003) the two upper figures illustrate the continuous displacement fields and the following two figures illustrate the discontinuous displacement field. Regarding the formulation by Mergheim, *et al.* (2005) the two upper figures illustrate the displacement field for the two “original” nodes 1 and 2 while figure 3 and 4 depict the displacement fields for the dual nodes 1\* and 2\*. The lower figure in each column illustrates how a displacement jump of magnitude one may be modeled by the different formulations

## 2. Enrichment of displacement field

The displacement field for a cracked element can be formulated as the sum of the continuous and the discontinuous displacement field as already illustrated in Fig. 1. The continuous displacement field is defined equally to the displacement field for an uncracked element, i.e., the displacement

field may be written

$$\mathbf{u}(x,y) = \mathbf{N}^c(x,y)\mathbf{v}^c + \mathbf{N}^d(x,y)\mathbf{v}^d \quad (1)$$

where  $\mathbf{v}^c$  and  $\mathbf{v}^d$  are the degree of freedom (dof) vectors while  $\mathbf{N}^c$  and  $\mathbf{N}^d$  are the interpolation matrices.  $c$  refers to continuous and  $d$  to discontinuous.

The element discontinuity interpolation matrix,  $\mathbf{N}^d$ , is chosen as suggested in Asferg, *et al.* (2004).

$$\mathbf{N}^d(x,y) = \sum_I H_I(x,y)\mathbf{N}_I^c(x,y) \quad (2)$$

where  $H_I(x,y)$  is the 2D Heaviside step function for node  $I$ . The step function  $H_I(x,y)$  is 0 on the same side of the discontinuity as node  $I$  and 1 on the other side.

Fig. 2 illustrates a discontinuous displacement field for a CST element cut by a crack while Fig. 3 illustrates two of the discontinuous displacement fields for a LST element. The left most subfigure in each figure shows the crack geometry, coordinates to the start and the endpoints are given in area coordinates, while the remaining subfigures show individual nodal discontinuous displacement fields.

From Fig. 2 and Fig. 3 it is seen that the choice of interpolation for the discontinuous displacement field ensures that the discontinuous contribution to the displacement field vanish at all element edges not cut by the discontinuity implying the discontinuous displacement field to be included only in elements cut by the crack.

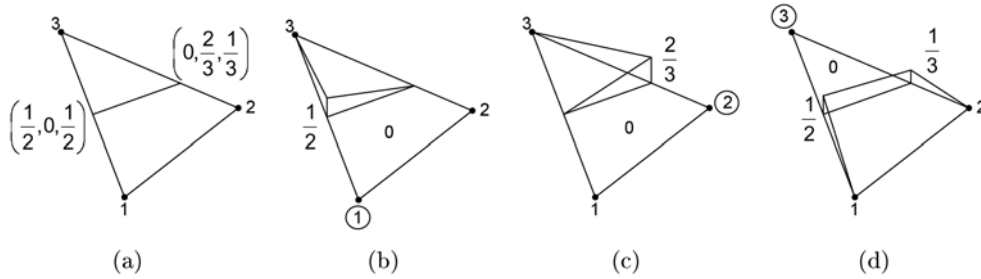


Fig. 2 Example of the enrichment of the displacement field for cracked CST element. (a) Crack geometry, (b), (c), (d) discontinuous displacement field for discontinuity dof's in node 1, 2 and 3

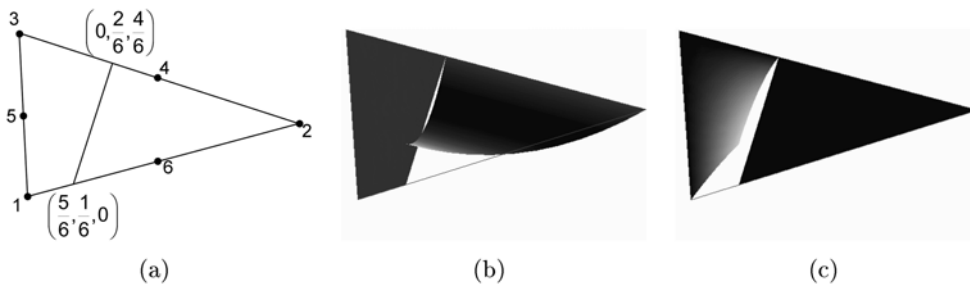


Fig. 3 Example of the enrichment of the displacement field for cracked LST element. (a) Crack geometry, (b) and (c) discontinuous displacement field for discontinuity dof's in node 1 respectively node 6

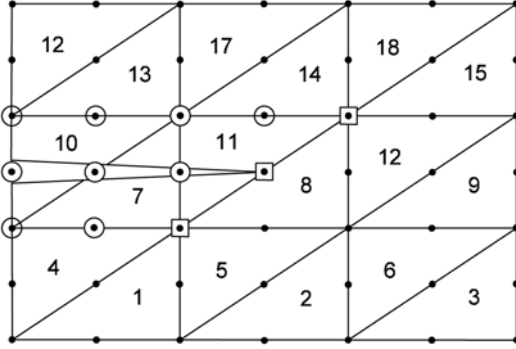


Fig. 4 Enrichment at system level for a mesh with LST elements. Nodes marked with a circle or a square are enriched. Discontinuity dof's in nodes marked with a square are set to zero

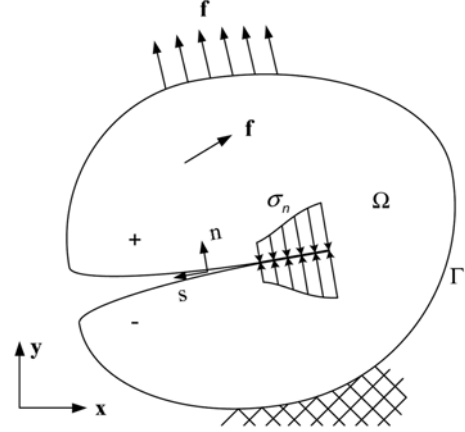


Fig. 5 Cohesive crack in a two dimensional domain with  $f$  representing both domain load and boundary load

Fig. 4 illustrates the enrichment at system level. Only nodes whose support is cut by the discontinuity are enriched. The discontinuity dof's located at the element edge where the crack tip is located have to be set to zero to ensure that the discontinuity at that edge is zero.

### 3. Variational formulation

Given a cohesive crack in a structure in a state of plane stress or plane strain described in a Cartesian coordinate system  $x,y$  (cf. Fig. 5), the arc length along the crack is termed  $s$ , and  $n,s$  is a curve linear coordinate system,  $n$  being normal to the crack face. The positive direction of  $s$  is seen on Fig. 5. The orientation of  $n$  determines the positive side of the crack. The stress state in the crack may be defined by the normal stress  $\sigma_n$  and the shear stress  $\tau_{ns}$  while work-conjugated generalized strains are the opening of the crack,  $\Delta u_n = u_n^+ - u_n^-$  and the slip in the crack,  $\Delta u_s = u_s^+ - u_s^-$ . A small strain / small displacement static theory is used and the material outside the crack is assumed linear elastic.

Let  $\llbracket \cdot \rrbracket$  denote a jump, then the stress increments  $d\sigma^{cr}$  across the crack surfaces are related to the increments in the displacement jump,  $d\llbracket \mathbf{u} \rrbracket$ , i.e., the separation of the crack surfaces through the tangential material stiffness matrix  $\mathbf{D}_T^{cr}$ .

$$\sigma^{cr}(\llbracket \mathbf{u} \rrbracket) = \begin{bmatrix} \sigma_n(\llbracket \mathbf{u} \rrbracket) \\ \tau_{ns}(\llbracket \mathbf{u} \rrbracket) \end{bmatrix} \quad \llbracket \mathbf{u} \rrbracket = \begin{bmatrix} \Delta u_n \\ \Delta u_s \end{bmatrix} \quad d\sigma^{cr}(\llbracket \mathbf{u} \rrbracket) = \mathbf{D}_T^{cr}(\llbracket \mathbf{u} \rrbracket) d\llbracket \mathbf{u} \rrbracket \quad (3)$$

For the uncracked part of the structure, the stress vector  $\sigma^T = [\sigma_x \ \sigma_y \ \tau_{xy}]$  and the strain vector  $\varepsilon^T = [\varepsilon_x \ \varepsilon_y \ \gamma_{xy}]$ , ( $\gamma_{xy} = 2\varepsilon_{xy}$ ) are defined as usual and related through the standard material stiffness matrix  $\mathbf{D}$ , specified below for an isotropic material in plane stress.

$$d\boldsymbol{\sigma} = \mathbf{D}d\boldsymbol{\varepsilon}, \quad \mathbf{D} = \frac{E}{1-\nu^2} \begin{bmatrix} 1 & \nu & 0 \\ \nu & 1 & 0 \\ 0 & 0 & \frac{1-\nu}{2} \end{bmatrix} \quad (4)$$

The virtual internal work-per-unit length of the crack  $\delta W_{cr}^i$  and the virtual internal work-per-unit area of the uncracked part of the structure  $\delta W_c^i$  may now be written,  $\delta$  referring to a virtual quantity

$$\begin{aligned} \delta W_{cr}^i &= \delta [\mathbf{u}]^T \boldsymbol{\sigma}^{cr} = \sigma_n \delta \Delta u_n + \tau_{ns} \delta \Delta u_s \\ \delta W_c^i &= \delta \boldsymbol{\varepsilon}^T \boldsymbol{\sigma} = \sigma_x \delta \varepsilon_x + \sigma_y \delta \varepsilon_y + \tau_{xy} \delta \gamma_{xy} \end{aligned} \quad (5)$$

For the entire structure the virtual internal and external work becomes

$$\begin{aligned} \delta W^i &= \int_{\Omega} \delta \boldsymbol{\varepsilon}^T \boldsymbol{\sigma} d\Omega + \int_{\Gamma} \delta [\mathbf{u}]^T \boldsymbol{\sigma}^{cr} d\Gamma \\ \delta W^e &= \int_{\Omega} \delta \mathbf{u}^T \mathbf{f} d\Omega + \int_{\Gamma} \delta \mathbf{u}^T \mathbf{f} d\Gamma \end{aligned} \quad (6)$$

where  $\mathbf{f}$  is the load on the structure.

By applying incremental quantities, the incremental stiffness relation, can obtained by:

$$\mathbf{K}_T \Delta \mathbf{V} = \int_{\Omega} \mathbf{N}^T \Delta \mathbf{f} d\Omega + \int_{\Gamma} \mathbf{N}^T \Delta \mathbf{f} d\Gamma \quad (7)$$

where  $\mathbf{V}$  is the system DOF vector and  $\Delta$  refers to an incremental quantity.

Special attention must be paid to the internal work, because the contribution from each element to the tangential stiffness  $\mathbf{K}_T$  depends on whether the element is cracked or not. The element tangential stiffness matrix,  $\mathbf{k}_T$ , for a cracked element is found by the following procedure. From Eqs. (1) and (2) the strain vector in a cracked element, except in the crack itself, is obtained

$$\boldsymbol{\varepsilon} = \mathbf{B}^c \mathbf{v}^c + \sum H_I \mathbf{B}_I^c \mathbf{v}_I^d = \mathbf{B}^c \mathbf{v}^c + \mathbf{B}^d \mathbf{v}^d \quad (8)$$

where  $\mathbf{B}^c$  and  $\mathbf{B}^d$  are the strain distribution matrices corresponding to the interpolation matrix  $\mathbf{N}^c$  respectively  $\mathbf{N}^d$ .

Due to the displacement field from the first term in Eq. (1) being continuous, the strains in the crack itself may be written as

$$[\mathbf{u}](s) = \mathbf{T}(\mathbf{N}_+^d(s) - \mathbf{N}_-^d(s)) \mathbf{v}^d = \mathbf{B}^{cr} \mathbf{v}^d \quad (9)$$

here,  $\mathbf{B}^{cr}$  is the strain distribution matrix in the crack,  $\mathbf{T}$  is the transformation matrix between the  $(x, y)$  and  $(n, s)$  coordinate systems, while  $\mathbf{N}_+^d$  and  $\mathbf{N}_-^d$  are the discontinuous interpolation matrices on the positive and negative sides of the crack respectively.

Applying the strain relations in Eqs. (8) and (9) when formulating the virtual incremental internal work,  $\mathbf{k}_T$  defined by  $\delta W^i = \delta \mathbf{v}^T \mathbf{k}_T \Delta \mathbf{v}$ , where  $\mathbf{v}^T = [\mathbf{v}^{cT} \ \mathbf{v}^{dT}]$ , is found to be

$$\mathbf{k}_T = \begin{bmatrix} \int \mathbf{B}^{cT} \mathbf{D} \mathbf{B}^c & \int \mathbf{B}^{cT} \mathbf{D} \mathbf{B}^d \\ \int \mathbf{B}^{dT} \mathbf{D} \mathbf{B}^c & \int \mathbf{B}^{dT} \mathbf{D} \mathbf{B}^d + \int_{cr} \mathbf{B}^{crT} \mathbf{D}^{cr} \mathbf{B}^{cr} \end{bmatrix} = \begin{bmatrix} \mathbf{k}^{cc} & \mathbf{k}^{cd} \\ \mathbf{k}^{dc} & \mathbf{k}^{dd} + \mathbf{k}_T^{cr} \end{bmatrix} \quad (10)$$

Due to a constant  $\mathbf{D}$ -matrix outside the crack, the stiffness contribution from the areas outside the

crack is constant and thus only the stiffness contribution from the crack itself is non-linear.

The element nodal forces,  $\mathbf{q}$ , depend like  $\mathbf{k}_T$ , on the crack opening, and they are determined analogous to  $\mathbf{k}_T$ . The contribution to  $\mathbf{q}$  from the crack,  $\mathbf{q}^{cr}$ , is found from the stresses in the crack. The stresses in the crack are related to the displacement jump across the crack according to Eq. (3). By adding this contribution to the contribution from the part of the element outside the crack,  $\mathbf{q}$  is obtained as

$$\mathbf{q} = \begin{bmatrix} \mathbf{k}^{cc} & \mathbf{k}^{cd} \\ \mathbf{k}^{dc} & \mathbf{k}^{dd} \end{bmatrix} \begin{bmatrix} \mathbf{v}^c \\ \mathbf{v}^d \end{bmatrix} + \mathbf{q}^{cr} \quad \text{where} \quad \mathbf{q}^{cr} = \int_{cr} \mathbf{B}^{crT} \begin{Bmatrix} \sigma_n \\ \tau_{ns} \end{Bmatrix} \quad (11)$$

## 4. Implementation

This section concerns the implementation of the XFEM scheme. First the condition for smooth crack closure is discussed. Hereafter the integration scheme for the enriched elements is presented. Then the criteria for the crack propagation are dealt with and finally the choice of the algorithm to solve the non-linear equations is discussed and the algorithm is given in a schematic form.

### 4.1. Conditions for smooth crack closure

In order to secure that the cohesive crack closes smoothly it is required that the stress intensity factors at the crack tip are vanishing (Vandewalle 2000). In Moës and Belytschko (2002) the mode I stress intensity factor,  $K_I$ , is evaluated applying a domain integral and when performing the iterations the load factor is determined such that  $K_I$  is zero at the crack tip. In the work by Zi and Belytschko (2003) it is stated that the equilibrium equations have been supplemented by a smooth crack closure condition at system level. Equivalent to the zero stress intensity factor condition, Zi and Belytschko require the stress projection in the normal direction of the crack to be equal to the tensile strength at the crack tip. However, adding an extra equation to be fulfilled at system level makes the structure of the algorithm different from the structure of most algorithms applied in commercial FEM codes. Investigations using cohesive interface crack elements by Stang, *et al.* (2006) show that smooth closure is automatically achieved in a finite element formulation with a stress criterion when a sufficient number of elements are applied. However, in the case considered in this paper, where the elements are either uncracked or fully cracked, it is just ensured that the stresses in the element next to the crack-tip element do not exceed the tensile strength. This approximately ensures smooth crack closure.

### 4.2. Integration of enriched elements

To ensure correct integration in elements cut by the discontinuity, integration must be performed independently on each side of the discontinuity. For integration purposes elements cut by the discontinuity are therefore subdivided into three triangular areas as illustrated in Fig. 6. In the case of CST elements one point Gauss quadrature is applied to each sub triangle and two integration points are used on the line of discontinuity. In the case of LST elements three point Gauss quadrature is applied in each sub triangle and three integration points are used along the line of discontinuity.

In elements not cut by the discontinuity standard Gauss quadrature is applied - one point Gauss quadrature is applied in the case of CST elements and three point Gauss quadrature is applied for LST elements.

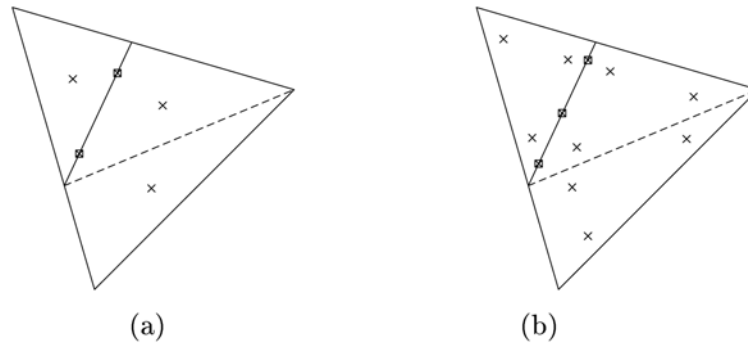


Fig. 6 Integration scheme for (a) CST and (b) LST element cut by discontinuity. Crosses marks integration point in continuum part of elements while crosses in boxes marks integration point on line of discontinuity for integration of traction forces

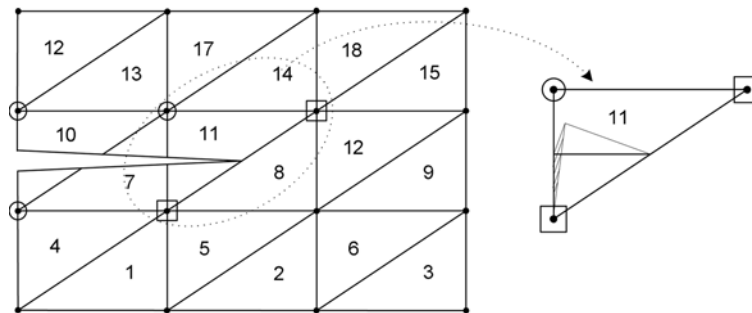


Fig. 7 Discontinuous displacement field in CST “tip” element

### 4.3. Crack growth

In the present work a discontinuity is introduced in the element, when the principal stress in the element exceeds the tensile strength of the material. The discontinuity is a straight line through the element originating from the point where the discontinuity ended in the previous cracked element. Hereby a continuous discontinuity is assured.

Concerning the crack growth direction different approaches have been considered. The first and simplest approach is local and rely only upon the stresses in the element that is located next to the tip-element (The element to become the next tip-element, element 8 in Fig. 7) for the determination of the crack growth direction. The discontinuity is grown perpendicular to the principal stress direction.

Several authors state that the local stresses in the next tip element can not be relied upon for computation of the crack growth direction and different nonlocal approaches are suggested. In Wells and Sluys (2001) the principal stress direction in the next tip element is computed from a non-local stress tensor calculated as a weighted average of stresses using a Gaussian weight function. Stresses in integration points within a radius of three times the typical element size are taken into account. In Moës and Belytschko (2002) the maximum hoop stress criterion is applied. The requirement for considering stresses in more than one element when computing the crack growth direction may appear when recalling the discontinuous displacement field in a cracked CST tip element c.f. Fig. 7.

Due to the discontinuous degrees of freedom in the nodes located on the crack tip edge being set equal to zero the crack tip element is not able to model the case, where equal stress are present at both sides of the discontinuity. This lack of capability to model correct stresses in the tip element influences the stresses in the next tip element and may call for more elements to be relied on for the computation of crack growth direction.

When a non-local stress tensor is applied in this work (only for CST elements), average nodal stresses are computed from element stresses in the elements sharing a given node - c.f. Eq. (12). All elements are assigned the same weight except previously cracked elements that are disregarded in the computation of the average nodal stresses due to the above illustrated bad stress field in the crack tip element. From the average nodal stresses a non-local stress tensor at the crack tip is interpolated by Eq. (13) and used for the determination of the crack growth direction. In Eq. (13)  $(\zeta_1, \zeta_2, \zeta_3)$  are the area coordinates to the crack tip.

$$\sigma_{node}^{ave} = \left( \sum_{i=1}^{n_{el}^{uncr}} \sigma_i \right) / n_{el}^{uncr} \quad (12)$$

$$\sigma_{tip}^{NL} = \begin{bmatrix} \sigma_x^{no1} & \sigma_x^{no2} & \sigma_x^{no3} \\ \sigma_y^{no1} & \sigma_y^{no2} & \sigma_y^{no3} \\ \tau_{xy}^{no1} & \tau_{xy}^{no2} & \tau_{xy}^{no3} \end{bmatrix} \begin{bmatrix} \zeta_1 \\ \zeta_2 \\ \zeta_3 \end{bmatrix} \quad (13)$$

Applying LST elements a non local procedure for computation of the crack growth direction is not necessary. The crack growth direction is computed from the principal stresses at the start point of the crack in the element.

#### 4.4. Algorithm

To remain within the framework of traditional FEM codes a general procedure, the orthogonal residual algorithm (Krenk 1995), was adopted for the XFEM scheme to solve the non-linear equations. The algorithm is summarized in Table 1.

As convergence criterion an energy criterion was applied and the elastic energy in the initial elastic load step was used as reference energy,  $E_{ref}$ . Further it may be noticed that it was chosen to implement the orthogonal residual algorithm in a Newton-Raphson style where the tangential stiffness matrix was updated in each iteration to take into account changes in crack opening and thereby also changes in the contribution from the enriched nodes during the iterations.

## 5. Numerical examples

To illustrate the capability of the suggested XFEM scheme two fracture mechanical benchmark tests, the three point beam bending test (TPBT) and the four point shear beam test (FPSB) has been considered. Results will be given for the TPBT applying CST as well as LST elements while only results applying LST elements will be given for the FPSB. Applying CST elements for the TPBT specimen local as well as nonlocal determination of crack growth direction will be considered and discussed.

Table 1 Orthogonal residual algorithm for XFEM

initial state:  $\mathbf{u}_0, \mathbf{f}_0, \Delta \mathbf{u}_0 = 0, E_{ref}, \Delta \mathbf{f}_0$

load increments  $n=1, 2, \dots, n_{max}$

$$\Delta \mathbf{u}_1 = \mathbf{K}_{T, n-1}^{-1} \Delta \mathbf{f}_n$$

$$\Delta \mathbf{u} = \min(1, u_{max} \|\Delta \mathbf{u}\|) \Delta \mathbf{u}$$

$$\Delta \mathbf{u}_0^T \Delta \mathbf{u} < 0 \text{ then } \Delta \mathbf{u} = -\Delta \mathbf{u}, \Delta \mathbf{f} = -\Delta \mathbf{f}$$

Iterations  $i=1, 2, \dots, i_{max}$

$$\Delta \mathbf{q} = \mathbf{q}(\mathbf{u} + \Delta \mathbf{u}) - \mathbf{f}_{n-1}$$

$$\zeta = \mathbf{q}^T \mathbf{u} / \mathbf{f}_n^T \Delta \mathbf{u}$$

$$\mathbf{r} = \zeta \Delta \mathbf{f}_n - \Delta \mathbf{q}$$

$$\mathbf{K}_{T, n} = \mathbf{K}_T(\mathbf{u} + \Delta \mathbf{u})$$

$$\delta \mathbf{u} = \mathbf{K}_{T, n}^{-1} \mathbf{r}$$

$$\delta \mathbf{u} = \min(1, u_{max} \|\delta \mathbf{u}\|) \delta \mathbf{u}$$

$$E_i = \mathbf{r}^T \delta \mathbf{u}$$

$$\varepsilon_i = E_i / E_{ref}$$

$$\Delta \mathbf{u} = \Delta \mathbf{u} + \delta \mathbf{u}$$

stop iteration when  $\varepsilon_i \leq$  stop value

$$\mathbf{u}_n = \mathbf{u}_{n-1} + \Delta \mathbf{u}_n$$

$$\mathbf{f}_n = \mathbf{f}_{n-1} + \zeta \Delta \mathbf{f}_n$$

$$\Delta \mathbf{u}_0 = \Delta \mathbf{u}$$

stop load increments when  $\|\mathbf{u}_n\| > u_{max}^{check}$

$\zeta$  is the optimal load scaling factor

$\mathbf{r}$  in the unbalanced force vector

$\delta \mathbf{u}$  is the displacement correction

$E_i$  is the residual energy

### 5.1. Three point beam bending test

The geometry of the TPBT specimen considered in this case is in accordance with the RILEM recommendations (Vandewalle 2000). The geometry is depicted in Fig. 8(a), the cross section of the beam being a square. For the material parameters standard values for a good quality concrete was chosen c.f. Table 2. A linear softening law as illustrated in Fig. 8(b) was applied for the normal stress in the crack. Considering a pure mode I problem the shear stiffness and the mixed mode stiffness terms for the crack were all set equal to zero, i.e., the tangential material stiffness matrix for the crack only holds one term different from zero:

$$D_{cr}^T = \begin{bmatrix} -f_t & 0 \\ \Delta u_{n,ult}^{cr} & 0 \\ 0 & 0 \end{bmatrix} \quad (14)$$

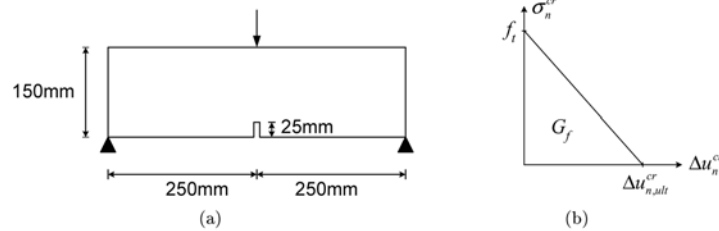


Fig. 8 (a) Geometry of TPBT specimen. (b) Applied linear softening curve

Table 2 Constitutive parameters

Parameter	Value
Young's modulus, $E_c$	37400MPa
Poisson's ratio, $\nu_c$	0.2
Tensile strength, $f_t$	3.5MPa
Fracture energy, $G_f$	160 N/m

### 5.1.1. Applying CST elements to model TPBT

Modeling the TPBT specimen applying CST elements structured as well as unstructured meshes were considered. Results will be given for two structured meshes, a 21 by 12 element c.f. Fig. 9(a), and a 25 by 24 element mesh. For both structured meshes results for local as well as non-local computation of crack growth direction will be given. The unstructured mesh, c.f. Fig. 9(b) consisted of 709 elements and results will only be given for the non-local crack growth computation. Note that for the structured meshes the notch is modeled as a predefined stress free discontinuity while in the unstructured mesh the notch is defined by the geometry of the mesh.

As reference for the XFEM computations the TPBT specimen was also modeled applying standard interface elements along a predefined crack path in the commercial code DIANA from TNO. Two meshes holding 24 respectively 48 elements over the beam height were considered for the DIANA computation.

Fig. 10 shows the load-deformation-response for the five considered XFEM computations and the two reference DIANA computations. The deformation is computed as the difference between the vertical displacement of the center point of the beam and the average vertical displacement of the mid points of the beam ends. Fig. 11 shows the predicted crack path for the 25 by 24 mesh applying local or nonlocal computation of the crack growth direction and the predicted crack path for the unstructured mesh.

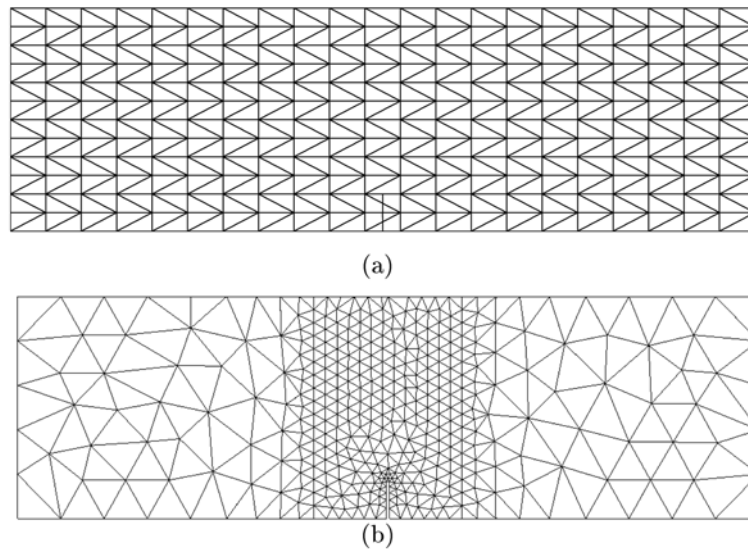


Fig. 9 (a) Structured mesh. (b) Unstructured mesh

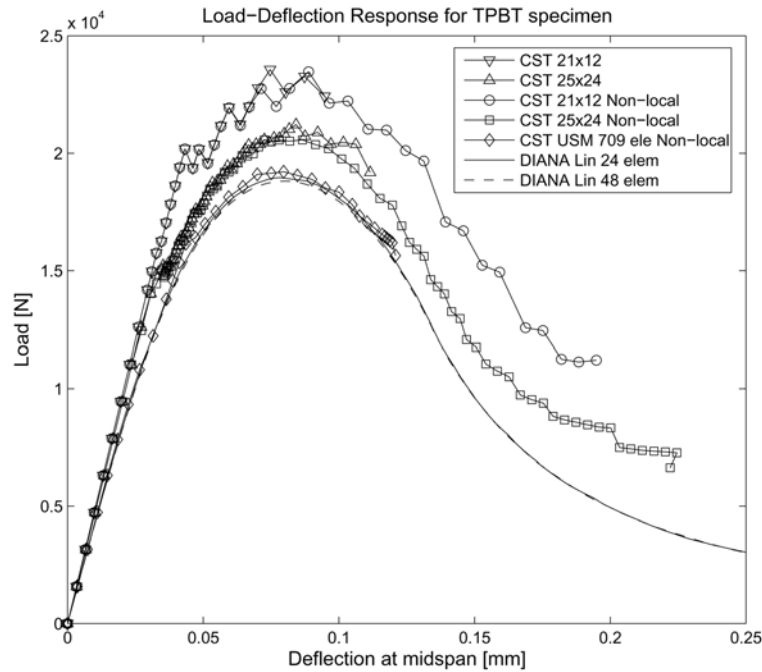


Fig. 10 Load-deformation-response for TPBT specimen modelled applying fully cracked CST elements

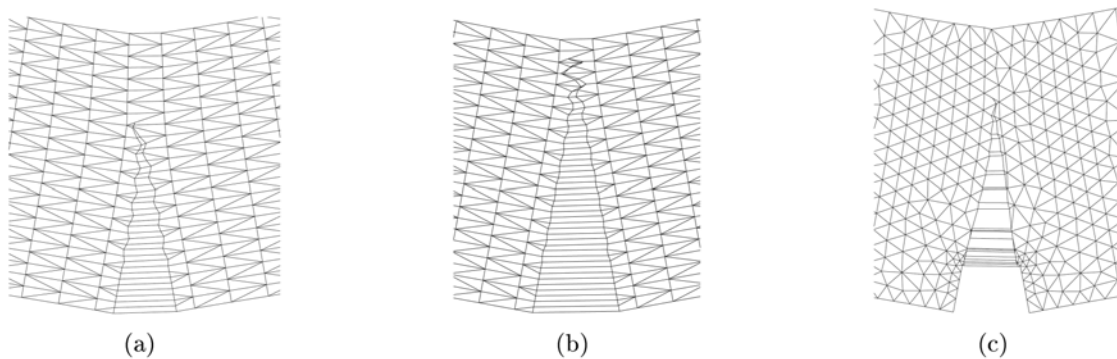


Fig. 11 Predicted crack path for: (a) 25 by 24 Mesh, local computation of crack growth direction. (b) 25 by 24 Mesh, non-local computation of crack growth direction (c) Unstructured mesh, non-local computation of crack growth direction

From the load-deformation-responses it is seen that the coarse structured mesh over predicts the load carrying capacity of the TPBT specimen with about 20% while the finer structured mesh overestimates the load carrying capacity with about 8%. The unstructured mesh predicts the maximum load carrying capacity well. Concerning the overall reproduction of the load-deformation-response it is seen that applying the local approach for the crack growth direction only the first part of the post peak response corresponding to the crack having propagated approximately through 2/3 of the beam height may be obtained. Applying the non-local approach for determining the crack

growth direction almost the full load-deformation response may be obtained - in Fig. 11(b) the crack has almost reached the top of the beam. The main reason for the bad prediction of the crack growth direction applying the local approach is the bad reproduction of the stresses in the tip element discussed in Section 4.3. The difference in stability of the determination of crack growth direction for the local versus the non-local approach is also evident from Fig. 11 (a) and (b). The non-local approach smoothes the crack path considerably compared to the local approach. The unstructured mesh captures the load carrying capacity well but is not able to reproduce the full load deformation response for the TPBT specimen with the applied non-local computation scheme. The use of non-local criteria for determination of crack growth direction is however seen as less appealing due to the required user interaction for determination of interaction radius that e.g., depends on the chosen element size and the actual structure considered. Use of a non local criterion to some extent violates the element local approach of the XFEM where everything is handled element locally.

### 5.1.2. Applying LST elements to model TPBT

Considering LST elements results are given for four structured meshes - a 11 by 6, a 15 by 9, the 21 by 12 and the 25 by 24 mesh. Only local computation of crack growth direction is considered. Fig. 12 compares the load-deformation response from the XFEM LST computations with the DIANA computation while Fig. 13 depicts the predicted crack patterns for the 21 by 12 and the 25 by 24 mesh.

From the load-deformation response it is seen that applying LST elements the overall behavior is predicted well by the 21 by 12 and the 25 by 24 mesh while the two coarsest meshes have troubles capturing the post peak response. Looking at the predicted crack paths it is seen that applying LST elements and hereby having more active discontinuity dof's, a more smooth crack path is achieved than for CST elements. However when the crack reaches the top of the beam and only a few

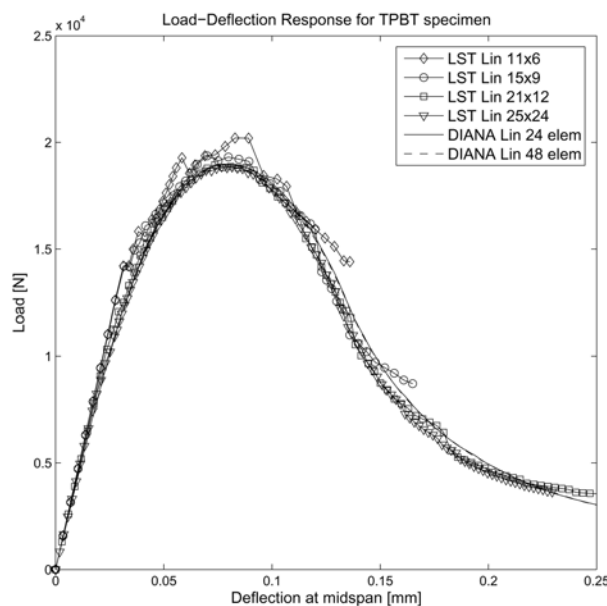


Fig. 12 Load-deformation-response for TPBT specimen modelled applying fully cracked LST elements

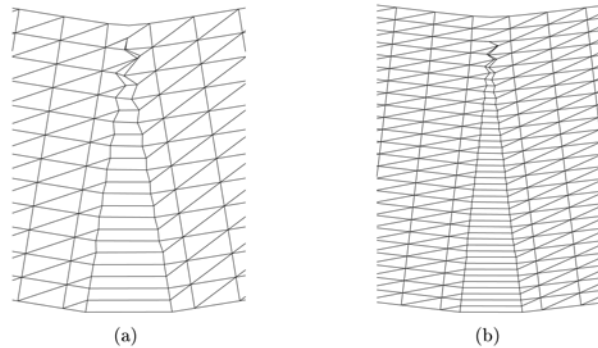


Fig. 13 Predicted crack path for LST computations of TPBT: (a) 21 by 12 Mesh. (b) 25 by 24 Mesh

elements remain uncracked the quality of the determined stress near the crack tip becomes low and hence influence the crack growth direction causing increasing tortuosity of the crack path. The conclusion is however that applying LST a sufficient accuracy concerning the crack growth direction is obtained by the local approach.

### 5.2. Four point shear beam

The four point shear beam serves to illustrate the capability of the suggested XFEM scheme to model curved cracks. The geometry of the four point shear beam (FPSB) - or the “double-edge notched specimen subjected to four point shear” is equivalent to the one investigated experimentally by Carpinteri, *et al.* (1992). In Carpinteri, *et al.* (1992) it is concluded that the FPSB may be modeled considering only mode I fracture, i.e. the shear stiffness in the crack may be ignored. The FPSB specimen was also analyzed by XFEM in Moës and Belytschko (2002). To maintain the basis for comparing the obtained results, fracture of the FPSB was also in the present case modeled considering only mode I fracture. The geometry of the test setup is shown in Fig. 14, while

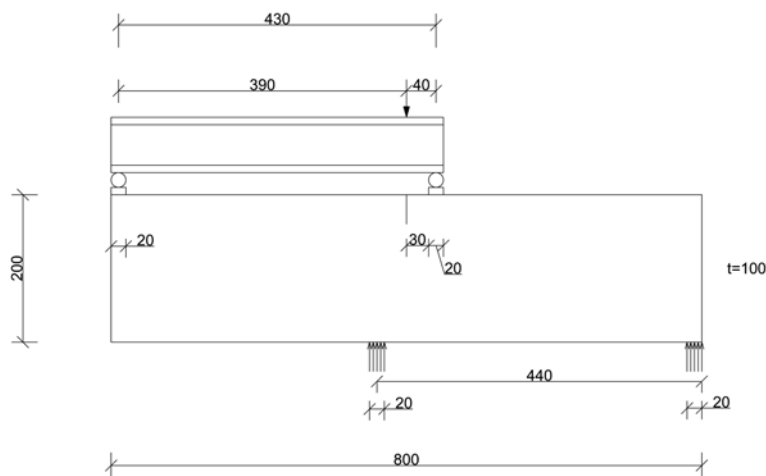


Fig. 14 Geometry of four point shear beam, all measures in mm

Table 3 Constitutive parameters FPSB

Parameter	Value
$E_c$	28000 MPa
$\nu_c$	0.1
$f_t$	2.4 MPa
$G_f$	145 N/m

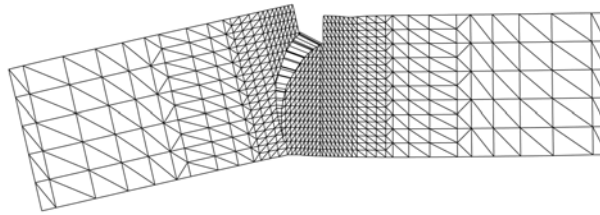


Fig. 15 Predicted crack path for FPSB specimen

constitutive parameters are given in Table 3. As for the TPBT specimen a linear softening curve (Fig. 8(b)) was applied.

A fairly coarse structured LST mesh, depicted in Fig. 15, consisting of 1222 elements and 2549 nodes was considered for the XFEM computation.

Fig. 15 depicts the computed crack path. The predicted crack path is in good agreement with the experimental findings in Carpinteri, *et al.* (1992). In Fig. 16 the computed load-deflection response is compared to the experimental load-deflection response obtained by Carpinteri, *et al.* (1992) and to the XFEM load-deflection response computed by Moës and Belytschko (2002). It is seen that the obtained results correlates well with the experimental results whereas some derivations are found when comparing to the results by Moës and Belytschko (2002).

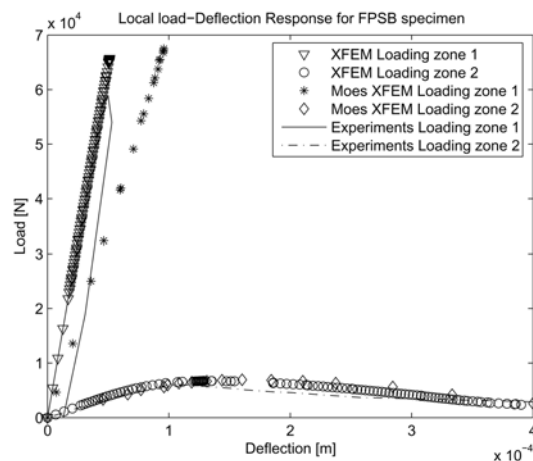


Fig. 16 Comparison of load-displacement response for FPSB obtained by present XFEM model, XFEM results by Moës and Belytschko (2002) and by experiments Carpinteri, *et al.* (1992). Loading zone 1 refers to the loading zone to the right in Fig. 14, while loading zone 2 refers to the left.

## 6. Conclusions

A direct enrichment of the displacement field has been implemented into an extended finite element scheme for modeling cohesive crack growth in concrete without remeshing. The XFEM scheme fits directly in the framework of standard finite element schemes. The XFEM scheme has been implemented for the three node constant strain triangle element (CST) and the linear strain six node triangle element (LST). Considering the CST element it was necessary to implement a nonlocal computation of crack growth direction to obtain good prediction of the crack path while for the LST element the crack path computation could be based on element local computations. Considering three point bending and four point shear, the efficiency of the suggested scheme was illustrated and it was found that even for relatively coarse meshes the scheme produces good results.

## References

- Asferg, J. L., Poulsen, P. N. and Nielsen, L. O. (2004), "Modeling of cohesive crack applying XFEM", *5th International PhD Symposium in Civil Engineering*, Walraven, J., Blaauwendraad, J., Scarpas, T. and Snijder, B. (Eds.), pages 1261-1269.
- Barenblatt, G. I. (1962), "The mathematical theory of equilibrium of cracks in brittle fracture", *Advances in Applied Mech.*, **7**, 55-129.
- Bažant, Z. P. and Oh, B. H. (1983), "Crack band theory for fracture of concrete", *Mater. Struct., RILEM*, **16**(93), 155-177.
- Belytschko, T. and Black, T. (1999), "Elastic crack growth in finite elements with minimal remeshing", *Int. J. Numer. Methods Eng.*, **45**(5), 601-620.
- Belytschko, T., Krongauz, Y., Organ, D., Fleming, M. and Krysl, P. (1996), "Meshless methods: an overview and recent developments", *Comput. Methods Appl. Mech. Eng.*, **139**, 3-47.
- Bouchard, P. O., Bay, F. and Chastel, Y. (2002), "Numerical modelling of crack propagation: automatic remeshing and comparison of different criteria", *Comput. Methods Appl. Mech. Eng.*, **192**, 3887-3908.
- Bouchard, P. O., Bay, F., Chastel, Y. and Tovina, I. (2000), "Crack propagation modelling using an advanced remeshing technique", *Comput. Methods Appl. Mech. Eng.*, **189**, 723-742.
- Carpinteri, A., Valente, S., Ferrara, G. and Melchiorri, G. (1992), "Is mode II fracture energy a real material property?", *Comput. Struct.*, **48**(3), 397-413.
- Daux, C., Moës, N., Dolbow, J., Sukumar, N. and Belytschko, T. (2000), "Arbitrary branched and intersecting cracks with the extended finite element method", *Int. J. Numer. Methods Eng.*, **48**, 1741-1760.
- Dugdale, D. S. (1960), "Yielding of steel sheets containing slits", *J. Mech. Phys. Solids*, **8**, 100-104.
- Hillerborg, A., Modéer, M. and Peterson, P.-E. (1976), "Analysis of crack formation and crack growth in concrete by means of fracture mechanics and finite elements", *Cement Concrete Res.*, **6**, 773-782.
- Jirásek, M. (2000), "Comparative study on finite elements with embedded discontinuities", *Comput. Methods Appl. Mech. Eng.*, **188**, 307-330.
- Jirásek, M. and Belytschko, T. (2002), "Computational resolution of strong discontinuities", in: H. Mang, F. Rammerstorfer, J. Eberhardsteiner (Eds.), *Proceedings of Fifth World Congress on Computational Mechanics, WCCM V*, Vienna University of Technology, Austria.
- Karihaloo, B. L. (1995), *Fracture Mechanics and Structural Concrete*. Longman Scientific and Technical.
- Karihaloo, B. L. and Xiao, Q. Z. (2002), "Modelling of stationary and growing cracks in FE framework without remeshing: a state-of-the-art review", *Comput. Struct.*, **81**, 119-129.
- Krenk, S. (1995), "An orthogonal residual procedure for nonlinear finite element equations", *Int. J. Numer. Methods Eng.*, **38**, 823-839.
- Melenk, J. M. and Babuška, I. (1996), "The partition of unity finite element method: basic theory and application", *Comput. Methods Appl. Mech. Eng.*, **139**, 289-314.

- Mergheim, J., Kuhl, E. and Steinmann, P. (2005) "A finite element method for the computational modeling of cohesive cracks", *Int. J. Numer. Methods Eng.*, **63**, 276-289.
- Moës, N. and Belytschko, T. (2002), "Extended finite element method for cohesive crack growth", *Eng. Fract. Mech.*, **69**, 813-833.
- Moës, N., Dolbow, J. and Belytschko, T. (1999), "A finite element method for crack growth without remeshing", *Int. J. Numer. Methods Eng.*, **46**, 131-150.
- Nielsen, M. P. (1999), *Limit Analysis and Concrete Plasticity*. CRC Press, second edition.
- Patzák, B. and Jirásek, M. (2004), "Adaptive resolution of localized damage in quasi-brittle materials", *J. Eng. Mech.*, **130**, 720-732.
- Stang, H., Olesen, J. F., Poulsen, P. N. and Dick-Nielsen, L. (2006), "Application of the cohesive crack in cementitious materials modelling", In Meschke, G. de Borst, R. Mang, H. and Bicanic, N., Editors, *Computational Modeling of Concrete Structures*, 443-449, Taylor & Francis.
- Stolarska, M., Chopp, D. L., Moës, N. and Belytschko, T. (2001), "Modeling crack growth by level sets in the extended finite element method", *Int. J. Numer. Methods Eng.*, **51**, 943-960.
- Sukumar, N., Moës, N., Moran, B. and Belytschko, T. (2000), "Extended finite element method for three dimensional crack modeling", *Int. J. Numer. Methods Eng.*, **48**, 1549-1570.
- Vandewalle, L. (2000), "Test and design methods for steel fiber reinforced concrete. Recommendations for bending test", *Mater. Struct.*, **33**, 3-5.
- Wells, G. and Sluys, L. (2001), "A new method for modeling of cohesive cracks using finite elements", *Int. J. Numer. Methods Eng.*, **50**(12), 2667-2682.
- Zi, G. and Belytschko, T. (2003), "New crack-tip elements for XFEM and applications to cohesive cracks", *Int. J. Numer. Methods Eng.*, **57**, 2221-2240.